Aquaporin 1 controls the functional phenotype of pulmonary smooth muscle cells in hypoxia-induced pulmonary hypertension

Schuoler, Claudio ; Haider, Thomas J ; Leuenberger, Caroline ; Vogel, Johannes ; Ostergaard, Louise ; Kwapiszewska, Grazyna ; Kohler, Malcolm ; Gassmann, Max ; Huber, Lars C ; Brock, Matthias

DOI: https://doi.org/10.1007/s00395-017-0620-7

Aquaporin 1 Controls the Functional Phenotype of Pulmonary Smooth Muscle Cells in Hypoxia-Induced Pulmonary Hypertension

Claudio Schuoler[1,2,3,#], Thomas J. Haider[1,2,#], Caroline Leuenberger[2,3], Johannes Vogel[1], Louise Ostergaard[1,2], Grazyna Kwapiszewska[4], Malcolm Kohler[2,3], Max Gassmann[1,2], Lars C. Huber[3,*], Matthias Brock[3,*]

1 Institute of Veterinary Physiology, Vetsuisse Faculty, University of Zurich, Zurich, Switzerland
2 Zurich Center for Integrative Human Physiology (ZIHP), University of Zurich, Zurich, Switzerland
3 Division of Pulmonology, University Hospital Zurich, University of Zurich, Zurich, Switzerland
4 Ludwig Boltzmann Institute for Lung Vascular Research, Graz, Austria
# these authors share first authorship
* these authors share senior authorship

Corresponding author:
Matthias Brock
Division of Pulmonology
University Hospital Zurich
Wagistrasse 14
8952 Schlieren
Switzerland
E-mail: matthias.brock@uzh.ch
Phone: 0041 44 556 31 60

Abstract

Aims: Vascular remodelling in hypoxia-induced pulmonary hypertension (PH) is driven by excessive proliferation and migration of endothelial and smooth muscle cells. The expression of aquaporin 1 (AQP1), an integral membrane water channel protein involved in the control of these processes, is tightly regulated by oxygen levels. The role of AQP1 in the pathogenesis of PH, however, has not been directly addressed so far. This study was designed to characterize expression and function of AQP1 in pulmonary vascular cells from human arteries and in the mouse model of hypoxia-induced PH.

Methods and Results: Exposure of human pulmonary vascular cells to hypoxia significantly induced the expression of AQP1. Similarly, levels of AQP1 were found to be upregulated in lungs of mice with hypoxia-induced PH. The functional role of AQP1 was further tested in human pulmonary artery smooth muscle cells demonstrating that depletion of AQP1 reduced proliferation, the migratory potential, and, conversely, increased apoptosis of these cells. This effect was associated with higher expression of the tumour suppressor gene p53. Using the mouse model of hypoxia-induced PH, application of GapmeR inhibitors targeting AQP1 abated the hypoxia-induced upregulation of AQP1 and, of note, reversed PH by decreasing both right ventricular pressure and hypertrophy back to the levels of control mice.

Conclusions: Our data suggest an important functional role of AQP1 in the pathobiology of hypoxia-induced PH. These results offer novel insights in our pathogenetic understanding of the disease and propose AQP1 as potential therapeutic *in vivo* target.

Keywords: Aquaporin 1, Pulmonary Hypertension, Hypoxia, Proliferation, Vascular Remodelling

Introduction

Pulmonary hypertension (PH) is the pathophysiological consequence of several diseases and is, in many cases, triggered or aggravated by hypoxia [26, 28, 30]. The pulmonary vasculature of PH patients is characterized by vasoconstriction, microthrombotic events and excessive remodelling of the small pulmonary arteries [9, 24]. Whereas acute hypoxia increases pulmonary pressure by calcium-mediated vasoconstriction of pulmonary vascular smooth muscle cells on the short term, conditions of chronic hypoxia, including many parenchymal lung disease, trigger mechanisms of remodelling that result in the development of irreversible pulmonary hypertension [37]. Vascular remodelling is due to migration and proliferation of cells within all layers of the vessel wall, most prominently however of pulmonary artery smooth muscle and endothelial cells [20]. Uncontrolled proliferation and resistance to apoptosis of these cells have also been described as neoplastic-like processes [29]. To date, vascular remodelling is not satisfyingly addressed by treatment [7].

The mammalian aquaporins (AQPs) are a class of water channels that regulate the rapid water movement across the plasma membrane in response to an osmotic gradient [18]. The AQP family consists of 13 different subsets (AQP0-12) so far which are expressed in multiple organs including the lungs. AQPs are involved in various physiological processes such as trans-epithelial fluid transport, cell migration, cell proliferation, and angiogenesis [35]. These processes are, probably by the action of AQPs, of major importance for the physiological adaption to hypoxia as well as in the pathophysiology of cancer[34] and hypoxia-related diseases [27].

A steadily growing number of studies emphasize that AQPs seem to be strongly involved in stress-induced tissue transformation processes. Recently, it was suggested that hypoxia modulates AQP1 expression in different organs, e.g. mouse lungs [1]. Moreover, in rat pulmonary artery smooth muscle cells, hypoxia selectively increased AQP1 protein levels and, in turn, migration of these cells [14]. These data suggest a possible link between the excessive vascular remodelling observed in patients with PH and both expression and function of AQP1.

However, the role of AQP1 in the pathobiology of vascular remodelling in PH has not been directly addressed so far. The present study was designed to investigate the expression and function of AQP1 in human vascular cells derived from pulmonary arteries and in the mouse model of hypoxia-induced PH. In detail, the functional consequence of altered AQP1 expression in human vascular cells was assessed with an emphasis on migration, proliferation and resistance to apoptosis. The physiological consequences of AQP1 depletion on haemodynamcis were further addressed *in vivo* by employing the hypoxia-induced mouse model of PH.

Methods

Animal Experiments

Male mice (C57BL/6, aged 12 weeks) were obtained from Charles River (Sulzfeld, Germany) and used for the hypoxia-induced PH mouse model as previously described in our publications [3, 4]. Briefly, the animals were randomized into a normoxic control group (n=8, room air, 21% O_2) and a hypoxic group (n=8, 10% O_2). Normobaric hypoxic condition was provided in a sealed glove-chamber connected to a gas mixer (Coy Laboratory Products, Grass Lake, MI, USA). Mice were assessed daily for activity and wellbeing. All animals had access to standard diet and tap water *ad libitum*. At day 35, after 5 weeks of hypoxic exposure, mice were anaesthetized (induction: 5% isoflurane, maintenance: 1.5-2% isoflurane and 100% O_2) and systemic arterial pressure (SAP) was measured in the isolated femoral artery. Next, right ventricular pressure (RVP) was evaluated as an endpoint measurement of PH, performed by right heart catheterization as previously described [10]. Mice were subsequently euthanized by cervical dislocation and lungs were collected for further analysis.

For treatment experiments, an additional mouse experiment was employed. Mice were divided into treatment and control groups (four groups of n=8 each). After three weeks of hypoxic exposure (10% O_2), the hypoxic mice were randomly assigned to three different groups to be further kept untreated or treated every four days by intraperitoneal (i.p.) injections with antisense oligonucleotides (GapmeRs) directed against AQP1 or GapmeR scrambled negative control (10mg/kg solved in sterile 0.9% NaCl). GapmeRs are short oligonucleotides modified with locked nucleic acids (LNA) in the flanking regions and DNA in a central gap (hence the name GapmeR). Application of GapmeR AQP1 results in RNase H-dependent degradation of complementary AQP1 RNA.

One mouse (hypoxic GapmeR negative control) died during the course of the experiment. Two weeks later, mice were analysed for RVP. The RVP of two hypoxic GapmeR AQP1 mice could not be measured since these mice died during right heart catheterization. Afterwards, animals were euthanized and lungs were harvested. To assess right ventricular hypertrophy, the ratio between right ventricular to left ventricular diameter including interventricular septum (RV/(LV+S)) was calculated based on the average of 3 linear diameter measurements across each heart section. All animal experiments were approved by the Cantonal Veterinary Office Zurich (approval numbers 151/2012 and 212/2014) and performed according to the guidelines from Directive 2010/63/EU of the European Parliament.

Cell Culture

Human pulmonary artery smooth muscle (HPASMC) (ScienCell, Carlsbad, CA, USA; donor #1 and #2) and human pulmonary artery endothelial cells (HPAEC) (ScienCell, Carlsbad, CA, USA; donor #1, and PromoCell, Heidelberg, Germany; donor #2) derived from two healthy donors were expanded in cultures according to the manufacturer's instructions. Cells were incubated in a humidified atmosphere at 37°C and 5% CO_2. In all experiments, one batch of cells with passage number between two and eight was used. Cells were seeded and allowed to settle for at least 12h before being transfected or exposed to hypoxia. Hypoxic experiments (1% O_2) were carried out over different time points (e.g. functional assays for 48h) in an O_2 adjustable incubator (Binder, Tutlingen, Germany) maintained at 37°C with 5% CO_2.

Transient Transfection of Primary Cultured Cells

For manipulation of endogenous levels of AQP1, HPASMC were transfected with GapmeR targeting AQP1 or GapmeR negative control (25nmol/L) using Lipofectamine 2000 transfection reagent (Life Technologies, Zug, Switzerland) according to the manufacturer's protocol. Cell culture grade GapmeR inhibitors were obtained from Exiqon (Vedbaek, Denmark) and their sequences are listed in Supplementary Table 1. Following an incubation period of 24 or 48h, cells were either harvested for gene expression analysis or prepared for functional assays.

Plasmid Construction and Overexpression

Conventional PCR was used to amplify the coding sequence of AQP1 (809bp) out of cDNA from HPASMC. The obtained PCR product was digested with *HindIII* and *XhoI* and subsequently cloned

into pcDNA 3.1(+) vector (Invitrogen, Basel, Switzerland). Successful insertion of AQP1 was confirmed by Sanger sequencing (Microsynth, Balgach, Switzerland). Primers used for cloning are provided in Supplementary Table 2. To overexpress AQP1, HPASMC were transfected either with 0.25µg pcDNA_AQP1 or its corresponding empty vector, which served as a negative control, using electroporation technique (Amaxa Nucleofactor kit, Lonza, Basel, Switzerland). Subsequently, after 48h, cells were harvested and gene overexpression was analysed by Western blotting or cells were prepared for migration and proliferation assays.

Quantitative Real-Time PCR (qPCR) Analysis

Total RNA of cultured cells or murine lung tissue samples were purified using the Quick-RNA MiniPrep kit (Zymo Research, Freiburg im Breisgau, Germany) or the miRNeasy Mini kit (Qiagen, Hombrechtikon, Switzerland), respectively. Quality of isolated RNA was assessed by spectrophotometric analysis (Nanodrop, Wilmington, DE, USA). Isolated RNA was reverse-transcribed using random hexamers and GoScript reverse transcriptase (both from Promega, Dübendorf, Switzerland). Quantification of specific gene transcripts was performed by SYBR Green qPCR (Applied Biosystem StepOnePlus system, Life Technologies). To avoid amplification of genomic DNA, primers were designed to span an exon-exon junction. Sequences of primers used for gene expression analysis are listed in Supplementary Table 2. Specific amplification was verified performing melt curve analysis. Obtained expression levels of genes of interest were normalized to the expression of β-actin. Differential gene expression was calculated using the threshold cycle (C_t) method [25].

Western Blotting

For protein extraction, harvested cells and murine lung tissue samples were lysed or homogenized using sample loading buffer (62.5mM Tris-HCl, pH 6.8, 2% sodium dodecyl sulphate (SDS), 10% glycerol, 5mM β-mercaptoehtanol, bromphenolblue). Whole-cell lysates (30µg of protein) were separated by 12% sodium dodecyl sulphate polyacrylamide gel electrophoresis (SDS-PAGE) and proteins were transferred by electroblotting to a nitrocellulose membrane (Whatman, GE Healthcare Life Sciences, Little Chalfont, UK). Membranes were blocked with 5% dry milk in Tris-buffered saline containing 0.1% Tween 20 (TBS-T) and incubated over night at 4°C with the following primary antibodies: anti-AQP1 (rabbit monoclonal, #ab168387, Abcam, Cambridge, UK), anti-hypoxia-inducible factor 1 alpha (HIF-1α) (rabbit polyclonal, #NB100-479, Novus Biologicals, Littleton, CO, USA), anti-p53 (mouse monoclonal, #sc-126, Santa Cruz Biotechnology, Dallas, TX, USA), and anti-β-actin (mouse monoclonal, #A2228, Sigma-Aldrich, Buchs SG, Switzerland), respectively. β-actin was used as a housekeeping protein for normalization. Bands were detected using species-specific secondary antibodies conjugated to horseradish peroxidase (Dako Agilent Technologies, Glostrup, Denmark). Calculation of the expression of proteins was performed using Adobe Photoshop CS5.1 software (Adobe Systems Incorporated, San Jose, CA, USA) via pixel quantification of the electronic image.

Migration Assay

Migration of HPASMC was addressed according to a modified *in vitro* wound-healing assay. Briefly, 30'000 cells were seeded on each side of an Ibidi culture insert µ-dish (Ibidi, Munich, Germany) for live cell analysis and transfected with GapmeR targeting AQP1 or scrambled negative control as described above. In addition, HPASMC were transfected with AQP1 overexpressing vector (pcDNA_AQP1) as stated above. Cells were allowed to grow to confluence for 24h and afterwards, inserts were removed with sterile tweezers to create a cell-free gap of approximately 500µm width. The closure of the wound by migrating cells was quantitatively assessed at various time points after being photographed at 4x magnification under an inverted microscope (Olympus CKX41) as previously described [21]. The area of the initial wound was compared to the area of the healing wound at three different time points (3, 5, and 7h).

Proliferation and Apoptosis Assay

To assess the proliferation rate, HPASMC were seeded in a 96-well plate at a density of 5000 cells per well and transfected with GapmeR targeting AQP1 or scrambled negative control as described above. For AQP1 overexpression, 10'000 cells were used and transfected either with pcDNA_AQP1 or its

corresponding empty vector as mentioned above. After 24h, 5-bromo-2-deoxyuridine (BrdU) was added to each well and cells were incubated for an additional 24h. Incorporation of BrdU was detected using the colorimetric BrdU assay from Roche (Roche Diagnostics, Mannheim, Germany). To assess apoptosis, HPASMC were seeded in a 96-well plate at a density of 10'000 cells per well and transfected with GapmeR targeting AQP1 or scrambled negative control. After 48h, apoptosis was evaluated in unstimulated cells (spontaneous apoptosis) by measuring the activity of caspase 3 and 7 (Caspase-Glo 3/7 assay, Promega, Dübendorf, Switzerland) according to the manufacturer's protocol.

Statistics

All data are presented as mean ± standard deviation (SD). Parametric or non-parametric distribution of data was determined using the Kolmogorov-Smirnov test. Data comparison was performed using independent Student's t-test as well as Pearson's correlation for parametric samples. For comparing more than two sample groups, the one-way analysis of variance (ANOVA) with Tukey *post hoc* test for parametric samples and the Kruskal-Wallis test with Dunns *post hoc* test for non-parametric samples was used. Paired Student's t-test or repeated measures ANOVA was used with Tukey *post hoc* test to analyse functional assays and AQP1 gene expression levels (paired observations of the same subject). In all statistical analyses, two-sided tests were applied. Values of $p<0.05$ were considered to be statistically significant (*$p<0.05$, **$p<0.01$, ***$p<0.001$). The n number indicates independent experiments. All statistical calculations were performed using the software package GraphPad Prism Version 5.0a (GraphPad Software, San Diego, CA, USA).

Results

AQP1 expression is increased in the mouse model of hypoxia-induced PH.
The regulation of AQP1 by hypoxia was characterized in lung samples of the mouse model of hypoxia-induced PH. As presented in Figure 1a, mice exposed to chronic hypoxia showed a significant elevation in RVP compared to normoxic control mice (in mmHg: hypoxic mice 45.45±3.63 vs. normoxic mice 30.83±2.60, $p<0.001$) indicating a successful *in vivo* application of the hypoxia-induced PH model. In lung tissue obtained from these mice, mRNA levels of AQP1 were significantly upregulated after hypoxia compared to normoxic control animals (by 1.31±0.14 fold change, $p<0.01$; Fig. 1b). These data were confirmed on protein level by Western blotting. AQP1 protein levels were significantly increased after exposure to chronic hypoxia (by 1.92±0.70 fold change, $p<0.01$; Fig. 1c). Since the levels of AQP1 were significantly upregulated under hypoxic conditions, a correlation analysis was performed showing a significant positive correlation of AQP1 protein levels with the RVP of experimental animals ($r=0.636$, $p<0.01$; Fig. 1d).

AQP1 is expressed in human pulmonary vascular cells.
In a next step, the basal expression levels of AQP1 in HPASMC and HPAEC, the two main cell types being involved in the process of vascular remodelling, were investigated. Both cell types express AQP1 on mRNA as well as protein levels. An increased mRNA expression of AQP1 in HPAEC was observed compared to HPASMC (e.g. ΔC_t of 8.74±2.01 in HPAEC donor #1 vs. ΔC_t of 15.09±0.56 in HPASMC donor #2, $p<0.05$; Fig. 2a). On protein level, there was no significant difference in the expression levels of AQP1 between the two donors of pulmonary vascular cell types (Fig. 2b).

Exposure to hypoxia drives the expression of AQP1 in human pulmonary vascular cells.
To further investigate the role of AQP1 in hypoxia-induced PH, pulmonary cells were exposed to hypoxia over different time points (1% O_2 for 2-72h). As indicated in Figure 3a, HPAEC showed the highest peak in AQP1 mRNA expression after 8h of hypoxic exposure (by 1.63±1.12 fold change, not significant; donor #1), whereas long-term hypoxia (24-72h) decreased mRNA levels with a significant reduction after 72h in donor #2 (reduction to 0.07±0.04, $p<0.05$). mRNA levels of AQP1 in HPASMC (donor #1) were significantly upregulated after 8h (by 2.18±0.80 fold change, $p<0.05$), 24h (by 2.87±0.89 fold change, $p<0.001$) and 48h (by 2.10±0.34 fold change, $p<0.05$) of hypoxic exposure. In donor #2, however, hypoxia did not change AQP1 mRNA levels (Fig. 3b). Protein expression of AQP1 in HPAEC was only found significant after 72h of hypoxia in donor #2 (by 1.88±0.49 fold change, $p<0.01$; Fig. 3c). In contrast, long-term hypoxia increased AQP1 protein levels in HPASMC, with a significant elevation after 48h (by 1.80±0.36 fold change, $p<0.05$; donor #1) and e.g. 72h (by 2.18±0.15 fold change, $p<0.001$; donor #2) of hypoxic exposure (Fig. 3d). Successful application of the hypoxic condition is indicated by representative Western blots of HIF-1α stabilization (Fig. 3c, d) as well as marked increase in mRNA levels of the HIF-1α inducible gene VEGFα (positive control, data not shown).

Silencing of AQP1 affects the phenotype of human pulmonary artery smooth muscle cells.
Since there was no difference in the amount of AQP1 protein expression in HPASMC and HPAEC (Fig. 2b) and the fact that HPASMC responded best to the hypoxic condition (Fig. 3), we focused on the latter cell type to continue with and to perform the following experiments and functional assays.

To evaluate the physiological role of AQP1 in the process of migration, proliferation and apoptosis in HPASMC, the endogenous expression of AQP1 was silenced by transfection with GapmeRs. As measured by qPCR, transfection of HPASMC with GapmeR targeting AQP1 significantly reduced the expression of AQP1 compared to non-transfected and negative control transfected cells in donor #1 (by 0.42±0.19 fold change, $p<0.01$; Fig. 4a). Additionally, these data were confirmed on protein level by Western blots demonstrating a significant decrease of AQP1 protein levels in donor #1 (by 0.66±0.13 fold change, $p<0.01$; Fig. 4b).
In terms of migration, as shown in Figure 4c, silencing of AQP1 in HPASMC significantly lowered the rate of healing in wound healing assays (e.g. after 7h of migration: GapmeR negative control

39.38%±5.00 vs. GapmeR AQP1 28.88%±7.86, p<0.001; donor #1). Representative pictures of migrated HPASMC are provided in Supplementary Figure 1. Likewise, as assessed by BrdU incorporation assay, transfection with GapmeR AQP1 resulted in a significantly reduced proliferation rate of HPASMC (donor #1) compared to non-transfected and GapmeR negative control transfected cells (in absorbance at 450nm: GapmeR negative control 1.76±0.17 vs. GapmeR AQP1 1.45±0.24, p<0.01; Fig. 4d). Conversely, HPASMC depleted of AQP1 showed significantly higher caspase 3/7 activity compared to both non-transfected and negative control transfected cells (in relative luminescence units: GapmeR negative control 4138±1106 vs. GapmeR AQP1 5558±1630, p<0.01; Fig. 4e) indicating a higher degree of spontaneous apoptosis when AQP1 is silenced. All results were confirmed using a second donor of HPASMC.

Silencing of AQP1 affects the phenotype of hypoxic human pulmonary artery smooth muscle cells.

To investigate the function of AQP1 under hypoxic conditions, HPASMC were transfected with GapmeR AQP1, exposed to hypoxia and, 48h later, their functional profile was assessed. As indicated in Figure 5a, inhibiting AQP1 resulted in significantly less hypoxic migration of HPASMC compared to non-transfected as well as negative control transfected cells (e.g. donor #1: rate of healing in % after 7h: Hx GapmeR negative control 31.88%±4.06 vs. Hx GapmeR AQP1 10.45%±4.36, p<0.001). Representative pictures of migrated HPASMC are provided in Supplementary Figure 2. Additionally, hypoxic HPASMC depleted of AQP1 showed significantly lower proliferation compared to control transfected cells (donor #1 in absorbance at 450nm: Hx GapmeR negative control 0.57±0.21 vs. Hx GapmeR AQP1 0.17±0.04, p<0.01; Fig. 5b). Of note, GapmeR neg. control transfected cells had significantly less proliferation rates compared to hypoxic non-transfected control cells. Moreover, in terms of apoptosis, HPASMC transfected with GapmeR AQP1 and exposed to hypoxia showed significantly higher caspase 3/7 activity in comparison to both control setups (donor #1 in relative luminescence units: e.g. Hx GapmeR negative control 1415±181 vs. Hx GapmeR AQP1 8538±767, p<0.001; Fig. 5c). Using a second donor of HPASMC, all results were confirmed. In summary, our experiments highlight the importance of AQP1 in the regulation of apoptosis, migration, and proliferation of HPASMC in normoxic as well as hypoxic conditions.

AQP1 controls the expression of p53 in human pulmonary artery smooth muscle cells.

To elucidate the molecular mechanism of AQP1 depletion in HPASMC, tumour suppressor and cell cycle inhibitor genes that have been previously implicated in the pathogenesis of PH were characterized in HPASMC transfected with GapmeR targeting AQP1. In detail, the mRNA levels of p53, BCL2, CDKN1A, and CDKN2A were measured by qPCR demonstrating a significant upregulation of p53 after transfection with GapmeR targeting AQP1 (by 1.43±0.15 fold change for donor #1 and by 3.18±0.54 fold change for donor #2, p<0.001; Fig. 6a), whereas no significant changes could be observed when the expression of the other genes was assessed (data not shown). Along that line, protein levels of p53 were significantly increased in both donor #1 by 2.97±0.77 fold change (p<0.001) and donor #2 by 5.18±3.18 fold change (p<0.05; Fig. 6b) when AQP1 was depleted in HPASMC compared to negative control transfected cells. Of interest, the expression of p53 was decreased in both HPASMC donors exposed to long-term hypoxia (e.g. 72h of hypoxia: 0.71±0.11 fold change for donor #1 and 0.55±0.20 fold change for donor #2, p<0.01; Fig. 6c). Western blots confirmed these results on protein level demonstrating a significant decrease of p53 after 72h of hypoxia in donor #1 and #2 (0.67±0.11 fold change and 0.52±0.05 fold change, respectively, p<0.05; Fig. 6d). These results highlight the regulation of the expression of p53 by AQP1 and hypoxia in HPASMC.

Enforced expression of AQP1 enhances migration and proliferation of human pulmonary artery smooth muscle cells.

To further confirm the role of AQP1 in the context of pulmonary vascular remodelling, AQP1 overexpression studies were performed in HPASMC. As demonstrated by the representative Western blot in Figure 7a, protein expression of AQP1 was significantly increased after transfection with pcDNA_AQP1 (donor #1 by 13.76±3.72 fold change, p<0.001). Regarding the migratory potential, HPASMC overexpressing AQP1 migrated faster than control cells as assessed by wound-healing assay (e.g. donor #1: rate of healing in % after 7h: pcDNA_empty 17.88%±5.52 vs. pcDNA_AQP1

24.83%±5.36, $p<0.001$; Fig. 7b). Representative pictures of migrated HPASMC are provided in Supplementary Figure 3. Moreover, as assessed by BrdU incorporation assay, HPASMC overexpressing AQP1 showed enhanced proliferation rates compared to HPASMC transfected with empty control vector (donor #1 in absorbance at 450nm: pcDNA_empty 0.57±0.17 vs. pcDNA_AQP1 0.77±0.18, $p<0.01$; Fig. 7c). All results were confirmed using a second donor of HPASMC.

Silencing of AQP1 reduces right ventricular pressure in the mouse model of hypoxia-induced PH.

The physiological consequences of AQP1 depletion via intervention experiments were further addressed *in vivo* by employing the hypoxia-induced mouse model of PH. The *in vivo* experiments were performed as described in the section 'Methods' (Fig. 8a).

As shown in Figure 8b, hypoxic control mice showed a significant increase in RVP compared to normoxic animals (in mmHg: 38.40±3.71 vs. 30.33±2.32, $p<0.05$) confirming the development of PH. Repeated i.p. injections of negative control GapmeR had no effect on RVP since RVP stayed significantly elevated in comparison with normoxic control. In contrast, treatment with GapmeR targeting AQP1 significantly reduced RVP in these mice compared to hypoxic GapmeR negative control mice (hypoxic GapmeR AQP1 mice 29.77±8.08 vs. hypoxic GapmeR negative control mice 41.00±3.40, $p<0.01$; Fig. 8b). Importantly, after treatment with GapmeR AQP1, RVP of these mice dropped to the same level as in normoxic control animals (Fig. 8b). Of note, systemic arterial pressure and haematocrit were not affected by GapmeR application indicating selective effects of GapmeR within the pulmonary circulation (Fig. 8c, d). Planimetric analysis of the ratio between right ventricular to left ventricular diameter including interventricular septum (RV/(LV+S)) showed a significant increase of the right ventricular volume following exposure to hypoxia (0.295±0.079) as compared to normoxic controls (0.183±0.039, $p<0.01$). Upon treatment with GapmeR against AQP1, the ratio was decreased (0.204±0.029, $p<0.05$; Fig. 8e).

In lung tissue collected from these mice, AQP1 mRNA levels were significantly elevated after hypoxic exposure compared to normoxic control mice (by 1.36±0.14 fold change, $p<0.01$; Fig. 8f) being in line with Figure 1b. Moreover, repeated i.p. injections of GapmeR targeting AQP1 significantly downregulated mRNA levels of AQP1 in lung tissue compared to hypoxic GapmeR negative control animals (hypoxic GapmeR negative control mice 1.24±0.28 fold change vs. hypoxic GapmeR AQP1 mice 0.97±0.14 fold change, $p<0.05$; Fig. 8f). Treatment with GapmeR AQP1 had no effect on mRNA levels of other AQPs expressed in the lung (AQP2-5), confirming specificity of the GapmeR design. Hypoxia, however, was able to significantly upregulate the expression of AQP4 and AQP5 (Supplementary Figure 4).

Affirming the results of the mRNA expression analysis, protein expression of AQP1 was found to be significantly upregulated in both hypoxic and hypoxic GapmeR negative control mice compared to normoxic control animals (hypoxic mice: by 2.77±1.23 fold change, hypoxic GapmeR negative control mice: by 2.90±0.87 fold change, $p<0.01$ and $p<0.001$, respectively; Fig. 8g). Administration of GapmeR AQP1 tended to reduce the protein expression of AQP1 to levels between normoxic and hypoxic animals (hypoxic GapmeR AQP1 mice 2.02±0.67 fold change vs. normoxic mice 1.00±0.36 fold change, not significant; Fig. 8g).

Discussion

AQP1 is known to be induced by hypoxia which itself might be both a causative factor for and a consequence of elevated pulmonary pressure. Of interest, however, the physiological consequence of the manipulation of AQP1 expression has not been described in the context of hypoxia-induced PH so far. In this study, we confirmed previous findings showing that hypoxic conditions increase the expression of AQP1 both *in vitro* and *in vivo* [14]. In addition, we demonstrated that manipulation of AQP1 affects the expression of the tumour suppressor gene p53 and influences the functional profile of pulmonary vascular cells on a migratory, proliferative and apoptotic level. By employing the hypoxia-induced PH mouse model, we found that silencing of AQP1 by a novel chimeric antisense oligonucleotide technology (GapmeRs) reversed established PH. Taken together, these findings represent the first direct link between AQP1 and PH and provide a novel interesting target to address pulmonary hypertension.

It was previously reported that AQP1 is induced by hypoxia in pulmonary artery smooth muscle cells. In detail, rat pulmonary artery smooth muscle cells exposed to hypoxia selectively increased AQP1 protein levels and, in turn, migration. Silencing of AQP1 via siRNA prevented the hypoxia-induced migration in these cells [13, 14]. Our initial experiments confirmed these findings by showing that the levels of AQP1 are increased by hypoxia in pulmonary artery smooth muscle cells. Of note, the observed induction of AQP1 could not be directly linked to the stabilization of HIF-1α suggesting the involvement of other mechanisms [1], for example the additional influx of calcium or interaction with microRNAs as suggested previously [14, 22]. The multi-factorial and complex induction of AQP1 by hypoxia is further emphasized by variable mRNA levels between the two donors. While the exact mechanisms behind these findings are elusive, high protein levels and functional data were consistently retrieved in long-term exposed HPASMC. Moreover, in lung tissue samples of animals exposed to hypoxia for five weeks, we found a significant increase in the expression of AQP1 compared to normoxic controls. Levels of AQP1 could be further correlated with pulmonary hemodynamics indicating that mice with higher AQP1 expression levels have increased right ventricular pressures and vice versa. Functional experiments and a subsequent treatment trial emphasized that this correlation might reflect causality and not only association.

Pulmonary artery smooth muscle cells showed an increased migratory response and dysregulation of the cell growth with development of a pro-proliferative and anti-apoptotic phenotype. Remodelling of small pulmonary arteries is the major factor in the pathobiology of PH and is, to date, not adequately addressed by modern PH-target therapies. Along that line, a recent publication demonstrated that genetic deletion of endothelial guanylyl cyclase-A receptor in mice caused pulmonary vascular remodelling, probably due to increased vascular cell proliferation, and PH already under normoxic conditions since the atrial natriuretic peptide (ANP) cannot exert its protective effects. This experimental study underpins the importance for novel strategies to target or even reverse pulmonary vascular remodelling and PH [38]. Vascular remodelling in the pulmonary circulation is characterized by migration of endothelial cells reflecting angiogenesis [36], formation of a “neo-intima” [20] and, most important, uncontrolled proliferation of smooth muscle cells [5]. These changes that result in progressive hyperplasia of the medial vessel layer and luminal obliteration have been described as neoplastic-like processes [29]. Since AQPs have been associated with malignant transformation and the development of cancer, our results might provide a novel mechanism explaining similar transformation in vessels of patients with PH. One of the best characterized tumour suppressor genes is p53 [32] and, in the context of PH, Jacquin et al. showed that p53 is found downregulated in the monocrotaline model of PH. Moreover, inactivation of p53 alone was sufficient to induce the development of experimental PH [11, 16]. Another study demonstrated that exogenous NO has an inhibitory effect on smooth muscle cell proliferation via induction of p53 and p21 [17]. In our experiments, silencing of AQP1 via GapmeRs resulted in higher mRNA and protein expression of p53. The interaction between p53 and AQP1 was further highlighted in hypoxic HPASMC showing decreased p53 levels with a concomitant increase of AQP1 expression (Figure 9). Additionally, enhanced p53 expression levels were found after silencing of AQP3 with shRNA in a non-small cell lung cancer (NSCLC) model, which was accompanied with suppressed tumour proliferation [39]. AQP3 knockdown reduced cellular glycerol content (AQP3 is a aquaglyceroporin) and mitochondrial

ATP formation, which, together with a reduction in PCNA levels, might contribute to the inhibitive effect on tumour proliferation. Of note, the importance of AQP1 for the vascular smooth muscle phenotype was highlighted in a study by Al Ghouleh et al. demonstrating that reactive oxygen species are channelled via AQP1 resulting in hypertrophy, however without affecting proliferation [2]. Furthermore, a study investigated the role of the C-terminal tail of AQP1 on migration and proliferation because the exact mechanism by which AQP1 facilitates these two processes remains unclear [13]. In this setting, the C-terminal was required since its deletion in AQP1 overexpressing rat smooth muscle cells abolished the effect on both migration and proliferation. They concluded that the possible AQP1-mediated mechanisms include association of factors or proteins with the C-terminal. The exact mechanism how AQP1 executes its function in this context, however, remains elusive and it will be difficult in general to unravel the underlying molecular mechanisms that act at the interface of hypoxia, AQP1, and PH.

Another link between AQP1 and proliferation was provided by data on adult carotid body cells, which were observed to proliferate less under hypoxic conditions when analysed in AQP1 knockout mice. Microarray data further revealed alterations in several proliferation-regulating genes suggesting that AQP1 modifies the expression of key cell cycle proteins [6].

In a next step, we tried to translate these *in vitro* findings by antagonizing AQP1 in an experimental model for PH. Animal models used to investigate PH have major limitations and only partially mimic human disease [8]. However, the hypoxia-induced mouse model is one of the best-established models for PH and, in the context of AQP1 that is strongly driven by hypoxic conditions, represents a suitable *in vivo* model. Silencing of AQP1 was achieved by administration of GapmeRs directed against AQP1. GapmeRs are single-stranded antisense oligonucleotides that catalyse the RNase H mediated degradation of complementary RNA targets and are active both *in vitro* and *in vivo*. To ensure enhanced stability and high target affinity, GapmeRs are composed of LNA-modified oligonucleotides flanking a central gap of DNA [33]. The usage of GapmeRs to target transcripts of genes of interest *in vivo* has been shown previously [31].

In this study, repeated intraperitoneal application of GapmeRs resulted in antagonizing of AQP1 and reversed the hypoxia-induced elevation of the pulmonary pressure. This is, to the best of our knowledge, the first report on the successful targeting of AQP1 *in vivo* through GapmeRs. In turn, as a consequence of reduced AQP1 expression in lung tissue, right ventricular pressure in animals exposed to hypoxia was reduced to levels of normoxic control animals. Performing additional experiments measuring mRNA levels of AQP2-5 in whole tissue from lungs in our GapmeR mouse setting of hypoxia-induced PH confirmed specificity of GapmeR for AQP1, where hypoxia was able to significantly upregulate the expression of AQP4 and AQP5 (Supplementary Figure 4). Furthermore, these results indicate that there was no compensational feedback regulation of other AQP subsets due to GapmeR treatment. A limitation of this study is the near absence of right ventricular hypertrophy in the Hx GapmeR neg. ctl group. This might be explained by a combination of methodical limitations of applied morphometric analysis and the relatively high biological variation, which was observed in our hypoxia-induced PH mouse model. Although this mouse model is frequently applied, it is supposed to be a mild one in terms of RVP increase, RVH, and pulmonary vascular remodelling [15]. However, RVP was significantly elevated in this group after hypoxic exposure. Newly established animal models for hypoxia-induced PH, e.g. the Sugen/hypoxia [19], were shown to induce a more pronounced pathological cardiorespiratory phenotype. Nevertheless, our data indicate that the pharmacological use of GapmeRs to target AQP1 reverses hypoxia-induced elevated pulmonary pressure and might treat vascular remodelling. The use of these novel antisense oligonucleotides could be limited by non-specific binding to proteins and off-target effects such as hepatotoxicity [12]. In our experiments, however, no such effects were observed indicating that GapmeR therapy is well tolerated and feasible.

In conclusion, this is the first report of AQPs in the context of PH. The identification of AQP1 expression and its functional characterization upon exposure to hypoxia unravels novel and important insights in the pathogenesis of pulmonary vascular remodelling. The therapeutic application of innovative antisense oligonucleotides resulted in successful antagonization of AQP1 and reversed experimental PH. However, it remains elusive at the moment whether these results might offer a future opportunity to target AQP1 in the lungs in order to prevent vascular remodelling in a selected cohort of patients with PH in the context of chronic lung disease.

Acknowledgements

The authors thank Rudolf Speich for his continuous support of our research, his commitment and enthusiasm to pulmonary hypertension and many invaluable inputs. We are deeply saddened by his unexpected death. Further, we would like to thank Giovanni Pellegrini from the Institute of Veterinary Physiology of the University of Zurich for his assistance with the animal samples.
This work was supported by the Swiss National Science Foundation [SNF grant 31003A 144212]; the Swiss Lung Association [LLS-Nr 2014-09]; the Hartmann Müller Foundation; and the Novartis Foundation for medical-biological Research [16B086].

Ethical Standards

All animal experiments were approved by the Cantonal Veterinary Office Zurich (approval numbers 151/2012 and 212/2014) and performed in accordance with the guidelines from Directive 2010/63/EU of the European Parliament as well as with the ethical standards laid down in the 1964 Declaration of Helsinki.

Conflict of Interest

The authors declare that they have no conflict of interest.

References

1. Abreu-Rodriguez I, Sanchez Silva R, Martins AP, Soveral G, Toledo-Aral JJ, Lopez-Barneo J, Echevarria M (2011) Functional and transcriptional induction of aquaporin-1 gene by hypoxia; analysis of promoter and role of Hif-1alpha. PLoS One 6:e28385 doi:10.1371/journal.pone.0028385
2. Al Ghouleh I, Frazziano G, Rodriguez AI, Csanyi G, Maniar S, St Croix CM, Kelley EE, Egana LA, Song GJ, Bisello A, Lee YJ, Pagano PJ (2013) Aquaporin 1, Nox1, and Ask1 mediate oxidant-induced smooth muscle cell hypertrophy. Cardiovasc Res 97:134-142 doi:10.1093/cvr/cvs295
3. Brock M, Haider TJ, Vogel J, Gassmann M, Speich R, Trenkmann M, Ulrich S, Kohler M, Huber LC (2015) The hypoxia-induced microRNA-130a controls pulmonary smooth muscle cell proliferation by directly targeting CDKN1A. Int J Biochem Cell Biol 61:129-137 doi:10.1016/j.biocel.2015.02.002
4. Brock M, Samillan VJ, Trenkmann M, Schwarzwald C, Ulrich S, Gay RE, Gassmann M, Ostergaard L, Gay S, Speich R, Huber LC (2014) AntagomiR directed against miR-20a restores functional BMPR2 signalling and prevents vascular remodelling in hypoxia-induced pulmonary hypertension. Eur Heart J 35:3203-3211 doi:10.1093/eurheartj/ehs060
5. Dorfmuller P, Humbert M (2012) Progress in pulmonary arterial hypertension pathology: relighting a torch inside the tunnel. Am J Respir Crit Care Med 186:210-212 doi:10.1164/rccm.201206-1049ED
6. Galan-Cobo A, Ramirez-Lorca R, Toledo-Aral JJ, Echevarria M (2016) Aquaporin-1 plays important role in proliferation by affecting cell cycle progression. J Cell Physiol 231:243-256 doi:10.1002/jcp.25078
7. Godinas L, Guignabert C, Seferian A, Perros F, Bergot E, Sibille Y, Humbert M, Montani D (2013) Tyrosine kinase inhibitors in pulmonary arterial hypertension: a double-edge sword? Semin Respir Crit Care Med 34:714-724 doi:10.1055/s-0033-1356494
8. Gomez-Arroyo J, Saleem SJ, Mizuno S, Syed AA, Bogaard HJ, Abbate A, Taraseviciene-Stewart L, Sung Y, Kraskauskas D, Farkas D, Conrad DH, Nicolls MR, Voelkel NF (2012) A brief overview of mouse models of pulmonary arterial hypertension: problems and prospects. Am J Physiol Lung Cell Mol Physiol 302:L977-991 doi:10.1152/ajplung.00362.2011
9. Huber LC, Bye H, Brock M (2015) The pathogenesis of pulmonary hypertension - an update. Swiss Med Wkly 145:w14202 doi:10.4414/smw.2015.14202
10. Huber LC, Ulrich S, Leuenberger C, Gassmann M, Vogel J, von Blotzheim LG, Speich R, Kohler M, Brock M (2015) microRNA-125a in pulmonary hypertension: Regulator of a proliferative phenotype of endothelial cells. Exp Biol Med (Maywood) 240:1580-1589 doi:10.1177/1535370215579018
11. Jacquin S, Rincheval V, Mignotte B, Richard S, Humbert M, Mercier O, Londono-Vallejo A, Fadel E, Eddahibi S (2015) Inactivation of p53 Is Sufficient to Induce Development of Pulmonary Hypertension in Rats. PLoS One 10:e0131940 doi:10.1371/journal.pone.0131940
12. Kakiuchi-Kiyota S, Koza-Taylor PH, Mantena SR, Nelms LF, Enayetallah AE, Hollingshead BD, Burdick AD, Reed LA, Warneke JA, Whiteley LO, Ryan AM, Mathialagan N (2014) Comparison of hepatic transcription profiles of locked ribonucleic acid antisense oligonucleotides: evidence of distinct pathways contributing to non-target mediated toxicity in mice. Toxicol Sci 138:234-248 doi:10.1093/toxsci/kft278
13. Lai N, Lade J, Leggett K, Yun X, Baksh S, Chau E, Crow MT, Sidhaye V, Wang J, Shimoda LA (2014) The aquaporin 1 C-terminal tail is required for migration and growth of pulmonary arterial myocytes. Am J Respir Cell Mol Biol 50:1010-1020 doi:10.1165/rcmb.2013-0374OC
14. Leggett K, Maylor J, Undem C, Lai N, Lu W, Schweitzer K, King LS, Myers AC, Sylvester JT, Sidhaye V, Shimoda LA (2012) Hypoxia-induced migration in pulmonary arterial smooth muscle cells requires calcium-dependent upregulation of aquaporin 1. Am J Physiol Lung Cell Mol Physiol 303:L343-353 doi:10.1152/ajplung.00130.2012

15. Maarman G, Lecour S, Butrous G, Thienemann F, Sliwa K (2013) A comprehensive review: the evolution of animal models in pulmonary hypertension research; are we there yet? Pulm Circ 3:739-756 doi:10.1086/674770
16. Mizuno S, Bogaard HJ, Kraskauskas D, Alhussaini A, Gomez-Arroyo J, Voelkel NF, Ishizaki T (2011) p53 Gene deficiency promotes hypoxia-induced pulmonary hypertension and vascular remodeling in mice. Am J Physiol Lung Cell Mol Physiol 300:L753-761 doi:10.1152/ajplung.00286.2010
17. Mizuno S, Kadowaki M, Demura Y, Ameshima S, Miyamori I, Ishizaki T (2004) p42/44 Mitogen-activated protein kinase regulated by p53 and nitric oxide in human pulmonary arterial smooth muscle cells. Am J Respir Cell Mol Biol 31:184-192 doi:10.1165/rcmb.2003-0397OC
18. Moon C, Preston GM, Griffin CA, Jabs EW, Agre P (1993) The human aquaporin-CHIP gene. Structure, organization, and chromosomal localization. J Biol Chem 268:15772-15778
19. Nicolls MR, Mizuno S, Taraseviciene-Stewart L, Farkas L, Drake JI, Al Husseini A, Gomez-Arroyo JG, Voelkel NF, Bogaard HJ (2012) New models of pulmonary hypertension based on VEGF receptor blockade-induced endothelial cell apoptosis. Pulm Circ 2:434-442 doi:10.4103/2045-8932.105031
20. Perros F, Dorfmuller P, Humbert M (2005) Current insights on the pathogenesis of pulmonary arterial hypertension. Semin Respir Crit Care Med 26:355-364 doi:10.1055/s-2005-916149
21. Reinhart-King CA (2008) Endothelial cell adhesion and migration. Methods Enzymol 443:45-64 doi:10.1016/S0076-6879(08)02003-X
22. Rutkovskiy A, Bliksoen M, Hillestad V, Amin M, Czibik G, Valen G, Vaage J, Amiry-Moghaddam M, Stenslokken KO (2013) Aquaporin-1 in cardiac endothelial cells is downregulated in ischemia, hypoxia and cardioplegia. J Mol Cell Cardiol 56:22-33 doi:10.1016/j.yjmcc.2012.12.002
23. Saadoun S, Papadopoulos MC, Hara-Chikuma M, Verkman AS (2005) Impairment of angiogenesis and cell migration by targeted aquaporin-1 gene disruption. Nature 434:786-792 doi:10.1038/nature03460
24. Schermuly RT, Ghofrani HA, Wilkins MR, Grimminger F (2011) Mechanisms of disease: pulmonary arterial hypertension. Nat Rev Cardiol 8:443-455 doi:10.1038/nrcardio.2011.87
25. Schmittgen TD, Livak KJ (2008) Analyzing real-time PCR data by the comparative C(T) method. Nat Protoc 3:1101-1108
26. Semenza GL (2011) Oxygen sensing, homeostasis, and disease. N Engl J Med 365:537-547 doi:10.1056/NEJMra1011165
27. She J, Bi J, Tong L, Song Y, Bai C (2013) New insights of aquaporin 5 in the pathogenesis of high altitude pulmonary edema. Diagn Pathol 8:193 doi:10.1186/1746-1596-8-193
28. Simonneau G, Gatzoulis MA, Adatia I, Celermajer D, Denton C, Ghofrani A, Gomez Sanchez MA, Krishna Kumar R, Landzberg M, Machado RF, Olschewski H, Robbins IM, Souza R (2013) Updated clinical classification of pulmonary hypertension. J Am Coll Cardiol 62:D34-41 doi:10.1016/j.jacc.2013.10.029
29. Soubrier F, Chung WK, Machado R, Grunig E, Aldred M, Geraci M, Loyd JE, Elliott CG, Trembath RC, Newman JH, Humbert M (2013) Genetics and genomics of pulmonary arterial hypertension. J Am Coll Cardiol 62:D13-21 doi:10.1016/j.jacc.2013.10.035
30. Souza R, Simonneau G (2014) Reply: pulmonary hypertension of sickle cell disease beyond classification constraints. J Am Coll Cardiol 63:2882-2883 doi:10.1016/j.jacc.2014.03.044
31. Straarup EM, Fisker N, Hedtjarn M, Lindholm MW, Rosenbohm C, Aarup V, Hansen HF, Orum H, Hansen JB, Koch T (2010) Short locked nucleic acid antisense oligonucleotides potently reduce apolipoprotein B mRNA and serum cholesterol in mice and non-human primates. Nucleic Acids Res 38:7100-7111 doi:10.1093/nar/gkq457
32. Suzuki K, Matsubara H (2011) Recent advances in p53 research and cancer treatment. J Biomed Biotechnol 2011:978312 doi:10.1155/2011/978312
33. Veedu RN, Wengel J (2010) Locked nucleic acids: promising nucleic acid analogs for therapeutic applications. Chem Biodivers 7:536-542 doi:10.1002/cbdv.200900343
34. Verkman AS (2012) Aquaporins in clinical medicine. Annu Rev Med 63:303-316 doi:10.1146/annurev-med-043010-193843

35. Verkman AS, Anderson MO, Papadopoulos MC (2014) Aquaporins: important but elusive drug targets. Nat Rev Drug Discov 13:259-277 doi:10.1038/nrd4226
36. Voelkel NF, Gomez-Arroyo J (2014) The role of vascular endothelial growth factor in pulmonary arterial hypertension. The angiogenesis paradox. Am J Respir Cell Mol Biol 51:474-484 doi:10.1165/rcmb.2014-0045TR
37. Ward JP, McMurtry IF (2009) Mechanisms of hypoxic pulmonary vasoconstriction and their roles in pulmonary hypertension: new findings for an old problem. Curr Opin Pharmacol 9:287-296 doi:10.1016/j.coph.2009.02.006
38. Werner F, Kojonazarov B, Gassner B, Abesser M, Schuh K, Volker K, Baba HA, Dahal BK, Schermuly RT, Kuhn M (2016) Endothelial actions of atrial natriuretic peptide prevent pulmonary hypertension in mice. Basic Res Cardiol 111:22 doi:10.1007/s00395-016-0541-x
39. Xia H, Ma YF, Yu CH, Li YJ, Tang J, Li JB, Zhao YN, Liu Y (2014) Aquaporin 3 knockdown suppresses tumour growth and angiogenesis in experimental non-small cell lung cancer. Exp Physiol 99:974-984 doi:10.1113/expphysiol.2014.078527

Figure Legends

Fig. 1 AQP1 expression is increased in the mouse model of hypoxia-induced PH. Mice were exposed to 10% O_2 for 5 weeks or kept under normoxia as controls. **(a)** Right ventricular pressure (RVP, in mmHg) measured by right heart catheterization in normoxic (Nx) and hypoxic (Hx) mice. Effect of hypoxia on mRNA **(b)** and protein **(c)** levels of AQP1 from lung homogenates measured by qPCR and Western Blot compared to normoxic animals. A representative blot is provided (30µg). **(d)** Correlation analysis of AQP1 protein expression with RVP of the corresponding mouse. n=8 mice per group. Statistical analysis by unpaired Student's t-test (a-c) and Pearson's correlation (d) (**p<0.01, ***p<0.001)

Fig. 2 AQP1 is expressed in human pulmonary vascular cells. Human pulmonary artery endothelial (HPAEC) and smooth muscle cells (HPASMC) express AQP1 on mRNA **(a)** as well as protein **(b)** level. A representative Western blot is shown (30µg). n=4-5 per group. Statistical analysis by Kruskal-Wallis test with Dunns *post hoc* test (a) and one-way ANOVA with Tukey *post hoc* test (b) (*p<0.05, **p<0.01)

Fig. 3 Exposure to hypoxia drives the expression of AQP1 in human pulmonary vascular cells. Two different donors for both vascular cell types were exposed to hypoxia (1% O_2 for 2-72h). **(a, b)** Effect of hypoxia on mRNA levels in HPAEC and HPASMC. **(c, d)** Effect of hypoxia on protein levels in HPAEC and HPASMC. Representative Western blots are provided (30µg). Immunodetection of HIF-1α was used to confirm successful application of hypoxia. n=5-6 per group. Statistical analysis by Kruskal-Wallis test with Dunns *post hoc* test (a, c) and one-way ANOVA with Tukey *post hoc* test (b, d) (*p<0.05, **p<0.01, ***p<0.001)

Fig. 4 Silencing of AQP1 affects the phenotype of HPASMC. Consequence of GapmeR transfection against AQP1 (25nmol/L) on both mRNA **(a)** and protein **(b)** levels in two donors of HPASMC compared to non-transfected and GapmeR negative control transfected cells. Representative Western blots are shown (30µg). Wound-healing **(c)** and BrdU incorporation **(d)** assays were performed assessing migration (rate of healing in %) and proliferation (absorbance at 450nm) of HPASMC after GapmeR AQP1 transfection. **(e)** Effect of AQP1 depletion in HPASMC on apoptosis as assessed by a luminescent assay that measures caspase-3 and -7 activities simultaneously (relative luminescence units). n=5-6 per group. Statistical analysis by repeated measures ANOVA with Tukey *post hoc* test (a and b top, c, d and e top) and paired Student's t-test (a, b, d and e bottom) (*p<0.05, **p<0.01, ***p<0.001)

Fig. 5 Silencing of AQP1 affects the phenotype of hypoxic HPASMC. Cells were transfected with GapmeR AQP1 (25nmol/L), exposed to hypoxia and, 48h later, their functional profile was assessed. Migratory **(a)** (rate of wound healing in %) and proliferative **(b)** (absorbance at 450nm) responses of HPASMC after depletion of AQP1 via GapmeR compared to control cells. **(c)** Apoptosis of HPASMC transfected with GapmeR targeting AQP1 as evaluated by a luminescent assay that measures caspase-3 and -7 activities simultaneously (relative luminescence units). n=5-6 per group. Statistical analysis by repeated measures ANOVA with Tukey *post hoc* test (a, b, c) (*p<0.05, **p<0.01, ***p<0.001).

Fig. 6 AQP1 controls the expression of p53 in HPASMC. Upon transfection with GapmeR targeting AQP1 (25nmol/L), mRNA **(a)** and protein **(b)** levels of p53 in two donors of HPASMC were evaluated relatively to control cells. Effect of hypoxia (1% O_2 for 2-72h) in HPASMC on mRNA **(c)** and protein **(d)** expression of p53. Representative Western blots are provided (30µg). n=5-6 per group. Statistical analysis by repeated measures ANOVA with Tukey *post hoc* test (a, b top), paired student's t-test (a, b bottom) and one-way ANOVA with Tukey *post hoc* test (c, d) (*p<0.05, **p<0.01, ***p<0.001)

Fig. 7 Enforced expression of AQP1 enhances migration and proliferation of HPASMC. Cells were transfected with a vector overexpressing AQP1 (pcDNA_AQP1). **(a)** AQP1 protein levels after

transfection with pcDNA_AQP1 (0.25µg) compared to empty control vector transfected cells (pcDNA_empty). A representative Western blot is shown (30µg). Migration **(b)** and proliferation **(c)** in AQP1 overexpressing HPASMC compared to control transfected cells as assessed by wound-healing (rate of healing in %) and BrdU incorporation (absorbance at 450nm) assays. n=5-6 per group. Statistical analysis by paired student's t-test (a, c) and repeated measures ANOVA with Tukey *post hoc* test (b) (*p<0.05, **p<0.01, ***p<0.001)

Fig. 8 Silencing of AQP1 reduces right ventricular pressure in the mouse model of hypoxia-induced PH. **(a)** Study design of the *in vivo* experiments. Four groups of eight animals each (n=7 for hypoxia GapmeR negative control) were used: three groups were employed in conditions at 10% O_2 for 5 weeks and, after 3 weeks, treated either with GapmeR negative control or GapmeR AQP1 (both 10mg/kg). Injections were performed intraperitoneally (i.p.) every fourth day. One group served as a normoxic control group. Hemodynamic assessment of the mouse model of hypoxia-induced PH shows **(b)** right ventricular pressure (RVP, in mmHg) measured by right heart catheterization (RHC), **(c)** systemic arterial pressure (SAP, in mmHg) and **(d)** haematocrit (%) in the three hypoxic (Hx) mouse groups compared to normoxic (Nx) animals. **(e)** Planimetric analysis of the ratio between the right to left ventricular volume including interventricular septum wall (RV/LV+S) (n=6-8). Effect of hypoxia and GapmeR treatment on AQP1 mRNA **(f)** and protein **(g)** expression in lung homogenates measured by qPCR and Western blot (n=7-8). A representative Western blot is provided (30µg). Statistical analysis by one-way ANOVA with Tukey *post hoc* test (b-g) (*p<0.05, **p<0.01, ***p<0.001)

Fig. 9 Proposed AQP1-mediated mechanism of vascular remodelling in the context of hypoxia-induced PH. Hypoxia-induced upregulation of AQP1 leads to a reduced expression of the tumour suppressor p53, promoting vascular smooth muscle cell proliferation (left side). As described by Saadoun et al. [23], AQP1 expression polarises to the leading edge of lamellipodia extension, facilitating water influx and cell migration (right side).

Figure 1

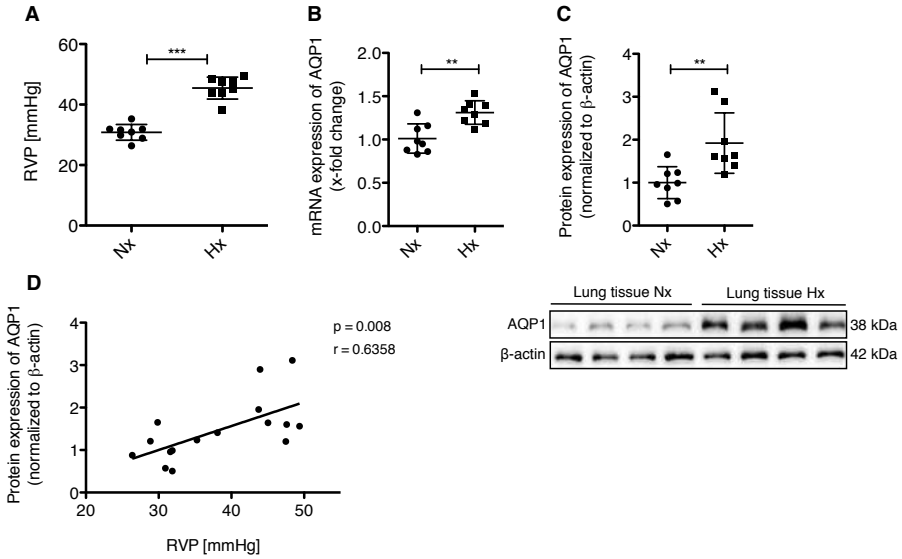
A
RVP [mmHg]
60
40
20
0
***
Nx
Hx
B
mRNA expression of AQP1
(x-fold change)
2.0
1.5
1.0
0.5
0.0
**
Nx
Hx
C
Protein expression of AQP1
(normalized to β-actin)
4
3
2
1
0
**
Nx
Hx
D
Protein expression of AQP1
(normalized to β-actin)
4
3
2
1
0
20
30
40
50
RVP [mmHg]
p = 0.008
r = 0.6358
Lung tissue Nx
Lung tissue Hx
AQP1
β-actin
38 kDa
42 kDa

Figure 2

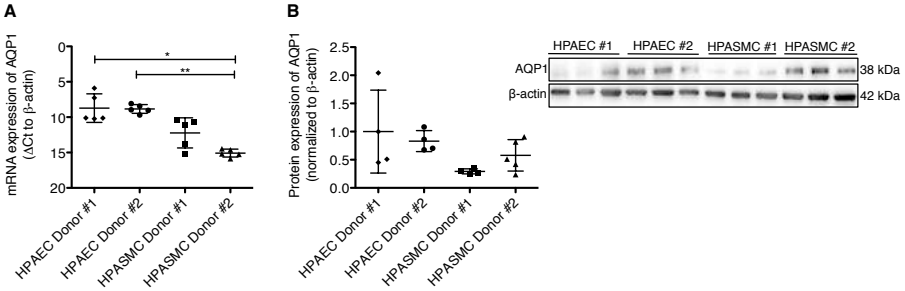
A
mRNA expression of AQP1
(ΔCt to β-actin)
0
5
10
15
20
*
**
HPAEC Donor #1
HPAEC Donor #2
HPASMC Donor #1
HPASMC Donor #2
B
Protein expression of AQP1
(normalized to β-actin)
2.5
2.0
1.5
1.0
0.5
0.0
HPAEC Donor #1
HPAEC Donor #2
HPASMC Donor #1
HPASMC Donor #2
HPAEC #1
HPAEC #2
HPASMC #1
HPASMC #2
AQP1
β-actin
38 kDa
42 kDa

Figure 3

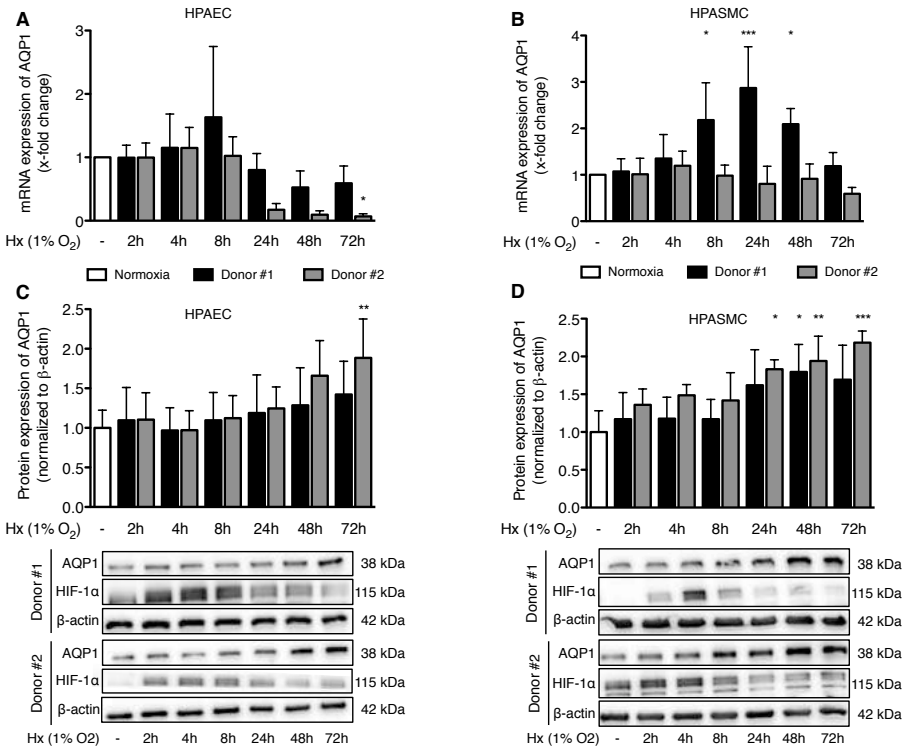
A
HPAEC
mRNA expression of AQP1 (x-fold change)
Hx (1% O2) - 2h 4h 8h 24h 48h 72h
Normoxia
Donor #1
Donor #2
B
HPASMC
mRNA expression of AQP1 (x-fold change)
C
HPAEC
Protein expression of AQP1 (normalized to β-actin)
D
HPASMC
Protein expression of AQP1 (normalized to β-actin)
Donor #1
Donor #2
AQP1
HIF-1α
β-actin
38 kDa
115 kDa
42 kDa

Figure 4

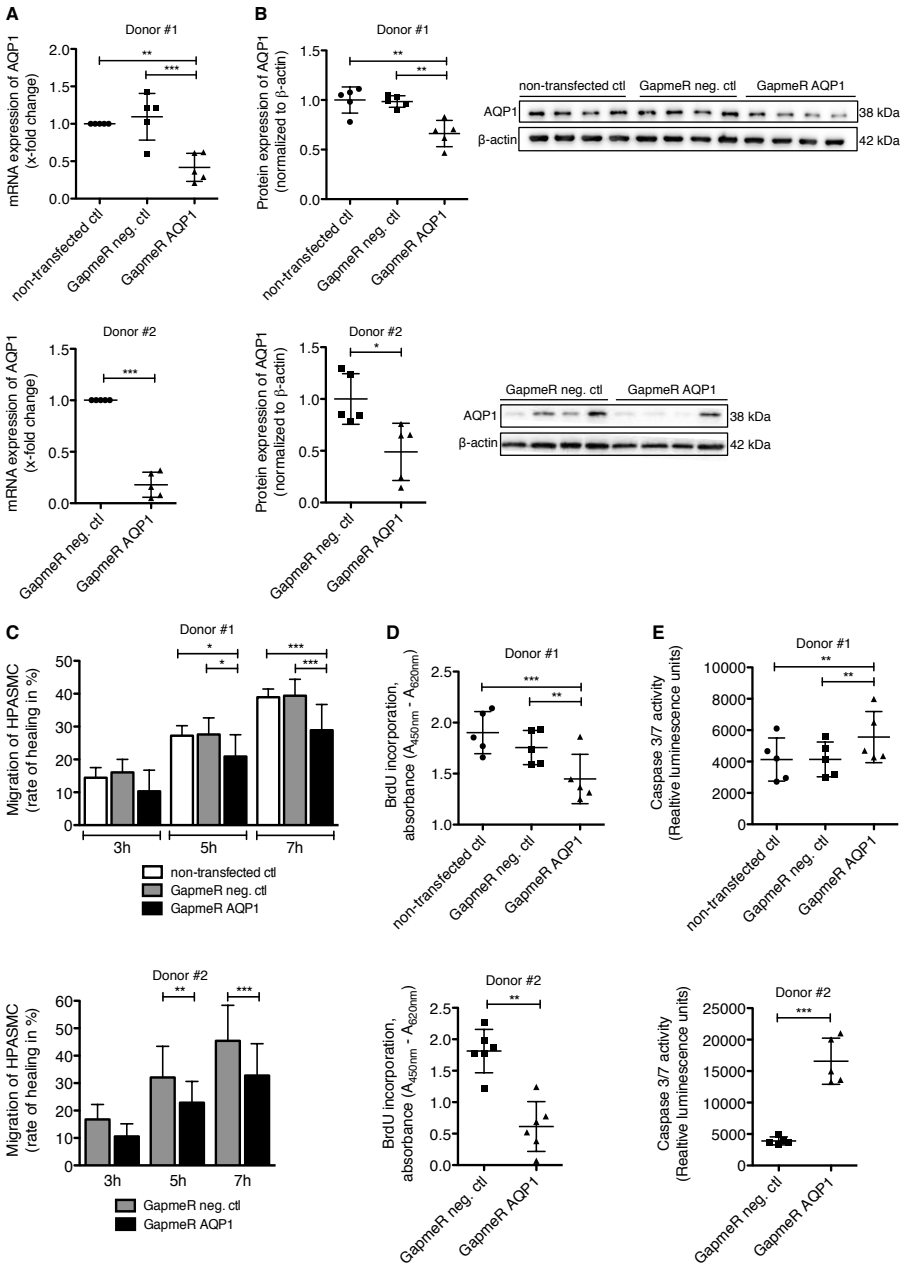
A
Donor #1
mRNA expression of AQP1 (x-fold change)
non-transfected ctl
GapmeR neg. ctl
GapmeR AQP1
B
Donor #1
Protein expression of AQP1 (normalized to β-actin)
non-transfected ctl
GapmeR neg. ctl
GapmeR AQP1
AQP1
β-actin
38 kDa
42 kDa
Donor #2
mRNA expression of AQP1 (x-fold change)
GapmeR neg. ctl
GapmeR AQP1
Donor #2
Protein expression of AQP1 (normalized to β-actin)
GapmeR neg. ctl
GapmeR AQP1
AQP1
β-actin
38 kDa
42 kDa
C
Donor #1
Migration of HPASMC (rate of healing in %)
3h
5h
7h
non-transfected ctl
GapmeR neg. ctl
GapmeR AQP1
Donor #2
Migration of HPASMC (rate of healing in %)
3h
5h
7h
GapmeR neg. ctl
GapmeR AQP1
D
Donor #1
BrdU incorporation, absorbance (A450nm - A620nm)
non-transfected ctl
GapmeR neg. ctl
GapmeR AQP1
Donor #2
BrdU incorporation, absorbance (A450nm - A620nm)
GapmeR neg. ctl
GapmeR AQP1
E
Donor #1
Caspase 3/7 activity (Realtive luminescence units)
non-transfected ctl
GapmeR neg. ctl
GapmeR AQP1
Donor #2
Caspase 3/7 activity (Realtive luminescence units)
GapmeR neg. ctl
GapmeR AQP1

Figure 5

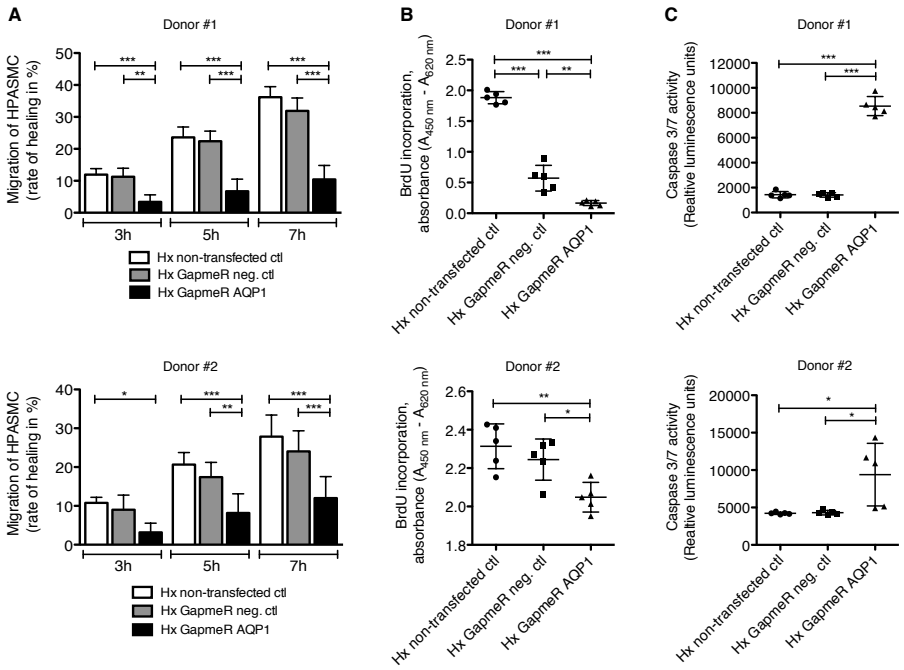
A
Donor #1
Migration of HPASMC (rate of healing in %)
3h
5h
7h
Hx non-transfected ctl
Hx GapmeR neg. ctl
Hx GapmeR AQP1
Donor #2
B
Donor #1
BrdU incorporation, absorbance (A450 nm - A620 nm)
Hx non-transfected ctl
Hx GapmeR neg. ctl
Hx GapmeR AQP1
Donor #2
C
Donor #1
Caspase 3/7 activity (Realtive luminescence units)
Donor #2

Figure 6

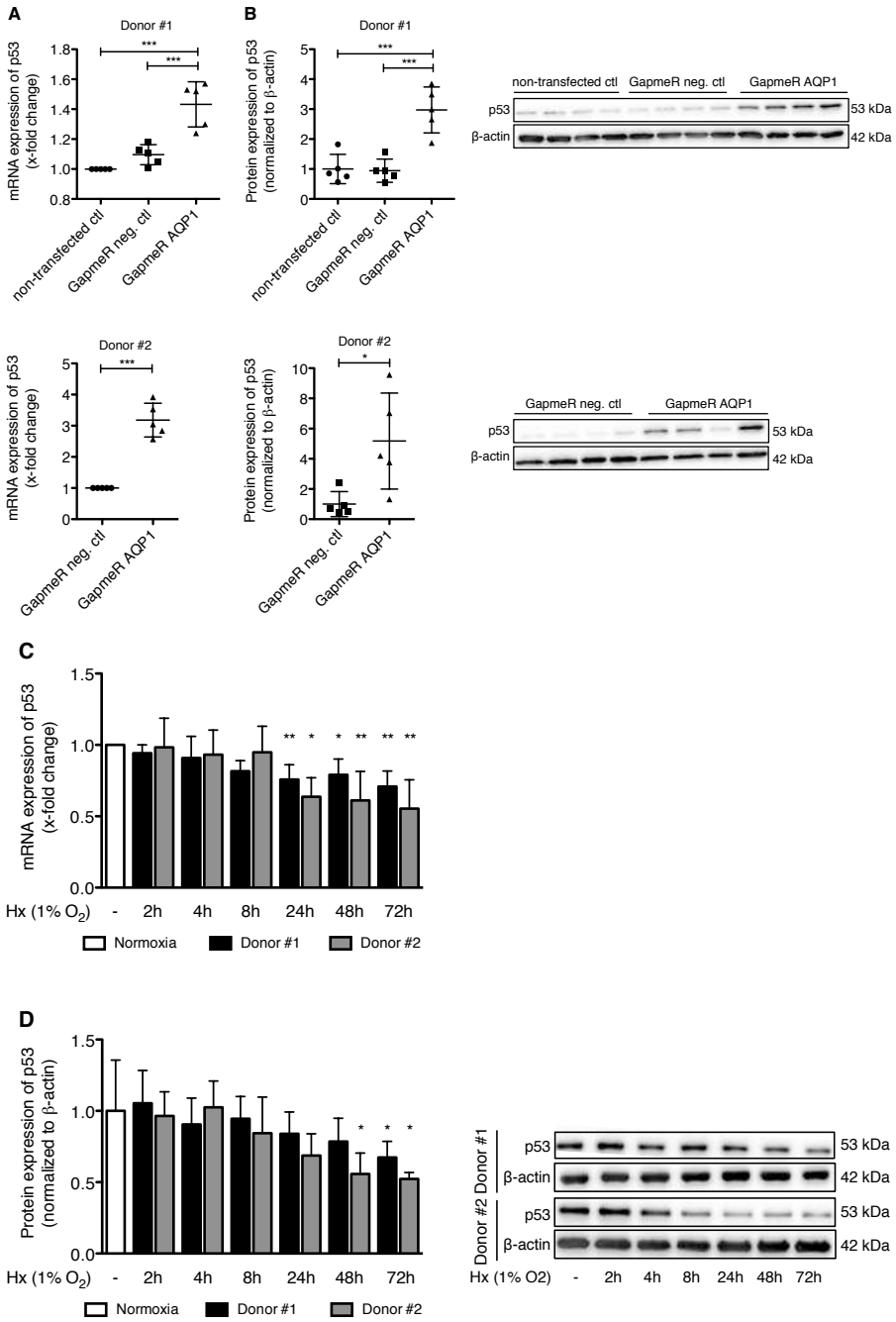
A
Donor #1
mRNA expression of p53 (x-fold change)
non-transfected ctl
GapmeR neg. ctl
GapmeR AQP1
B
Donor #1
Protein expression of p53 (normalized to β-actin)
non-transfected ctl
GapmeR neg. ctl
GapmeR AQP1
p53
β-actin
53 kDa
42 kDa
Donor #2
mRNA expression of p53 (x-fold change)
GapmeR neg. ctl
GapmeR AQP1
Donor #2
Protein expression of p53 (normalized to β-actin)
GapmeR neg. ctl
GapmeR AQP1
C
mRNA expression of p53 (x-fold change)
Hx (1% O2) - 2h 4h 8h 24h 48h 72h
Normoxia
Donor #1
Donor #2
D
Protein expression of p53 (normalized to β-actin)
Hx (1% O2) - 2h 4h 8h 24h 48h 72h
Normoxia
Donor #1
Donor #2
Donor #1
Donor #2
p53
β-actin
53 kDa
42 kDa
Hx (1% O2) - 2h 4h 8h 24h 48h 72h

Figure 7

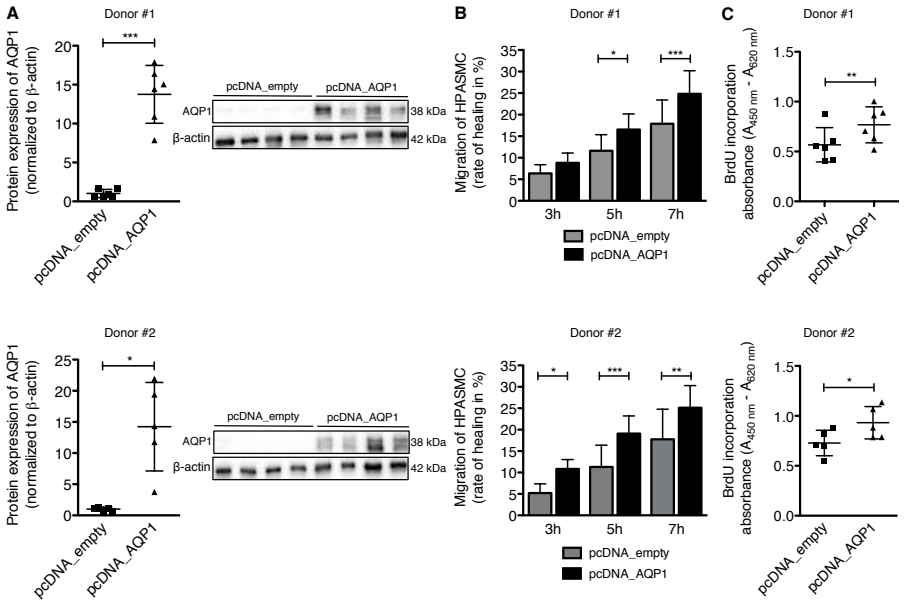
A
Donor #1
Protein expression of AQP1 (normalized to β-actin)
pcDNA_empty
pcDNA_AQP1
AQP1
β-actin
38 kDa
42 kDa
B
Donor #1
Migration of HPASMC (rate of healing in %)
3h
5h
7h
C
Donor #1
BrdU incorporation absorbance (A450 nm - A620 nm)
Donor #2

Figure 8

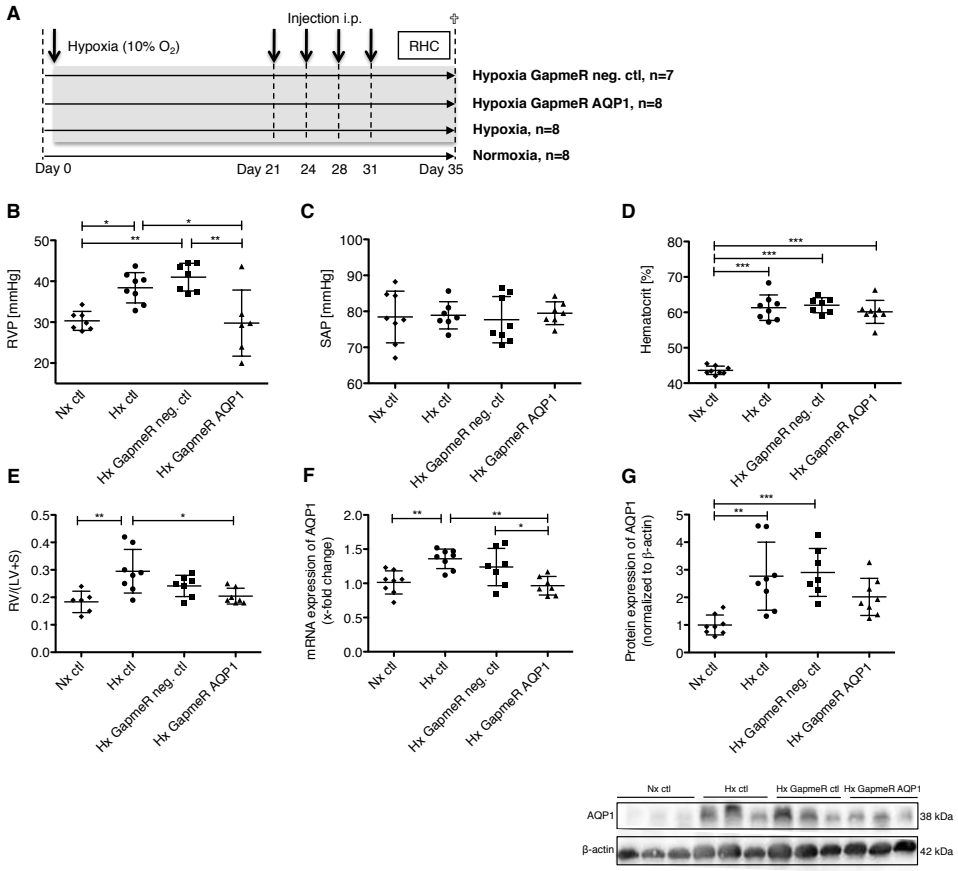
A
Injection i.p.
Hypoxia (10% O2)
RHC
Hypoxia GapmeR neg. ctl, n=7
Hypoxia GapmeR AQP1, n=8
Hypoxia, n=8
Normoxia, n=8
Day 0
Day 21
24
28
31
Day 35
B
RVP [mmHg]
C
SAP [mmHg]
D
Hematocrit [%]
E
RV/(LV+S)
F
mRNA expression of AQP1 (x-fold change)
G
Protein expression of AQP1 (normalized to β-actin)
Nx ctl
Hx ctl
Hx GapmeR neg. ctl
Hx GapmeR AQP1
AQP1
β-actin
38 kDa
42 kDa

Figure 9

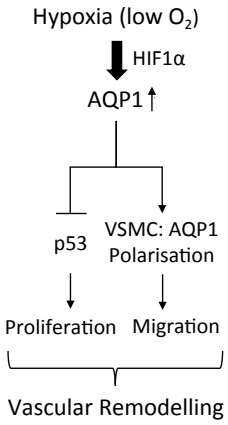
Hypoxia (low O_2)
HIF1α
AQP1↑
p53
VSMC: AQP1
Polarisation
Proliferation
Migration
Vascular Remodelling

SUPPLEMENTARY MATERIAL

Aquaporin 1 Controls the Functional Phenotype of Pulmonary Smooth Muscle Cells in Hypoxia-Induced Pulmonary Hypertension

Claudio Schuoler[1,2,3,#], Thomas J. Haider[1,2,#], Caroline Leuenberger[2,3], Johannes Vogel[1], Louise Ostergaard[1,2], Grazyna Kwapiszewska[4], Malcolm Kohler[2,3], Max Gassmann[1,2], Lars C. Huber[3,*], Matthias Brock[3,*]

1 Institute of Veterinary Physiology, Vetsuisse Faculty, University of Zurich, Zurich, Switzerland
2 Zurich Center for Integrative Human Physiology (ZIHP), University of Zurich, Zurich, Switzerland
3 Division of Pulmonology, University Hospital Zurich, University of Zurich, Zurich, Switzerland
4 Ludwig Boltzmann Institute for Lung Vascular Research, Graz, Austria
# these authors share first authorship
* these authors share senior authorship

Corresponding author:
Matthias Brock
Division of Pulmonology
University Hospital Zurich
Wagistrasse 14
8952 Schlieren
Switzerland
E-mail: matthias.brock@uzh.ch
Phone: 0041 44 556 31 60

Supplementary Table 1: Antisense LNA GapmeR sequences used for silencing of AQP1. + = prefix for LNA. Modification: phosphorothioate backbone.

GapmeR	Sequence	LNA content
GapmeR negative ctl	5' – +G+A+C TAA TGC ATT +A+T+C – 3'	6
GapmeR AQP1	5' – +T+G+T CAG AGT GTC +T+A+C – 3'	6

Supplementary Table 2: Primer sequences used for cloning of AQP1 and the validation of different genes by qPCR. hsa: *Homo sapiens*. mmu: *Mus musculus*.

AQP1 cloning	Primer forward	Primer reverse
Nested PCR	5' – ATG GCC AGC GAG TTC AAG – 3'	5' – CTA TTT GGG CTT CAT CTC C – 3'
Reverse PCR	5' – AAA CTT AAG CTT GCC GCC ATG GCC AGC GAG TTC AAG – 3'	5' – CTA GAC TCG AGC TAT TTG GGC TTC ATC TCC – 3'
Gene	**Primer forward**	**Primer reverse**
β-actin (hsa, mmu)	5' – TCA AGA TCA TTG CTC CTC CTG AG – 3'	5' – TCC TGC TTG CTG ATC CAC ATC – 3'
AQP1 (hsa)	5' – ACC TCC TGG CTA TTG ACT ACA C – 3'	5' – GGT TGC TGA AGT TGT GTG TGA TC – 3'
AQP1 (mmu)	5' – ACT TGG CCG CAA TGA CCT GG – 3'	5' – CAG AGT GCC AAT GAT CTC AAT GC – 3'
p53 (hsa)	5' – AGC CAC CTG AAG TCC AAA AAG – 3'	5' – CCC TTC TGT CTT GAA CAT GAG – 3'

Supplementary Figure 1: Representative pictures of HPASMC (donors #1 and #2) migrated for 7h in normoxia after transfection with GapmeR targeting AQP1 compared to non-transfected or GapmeR negative control transfected cells.

Donor #1

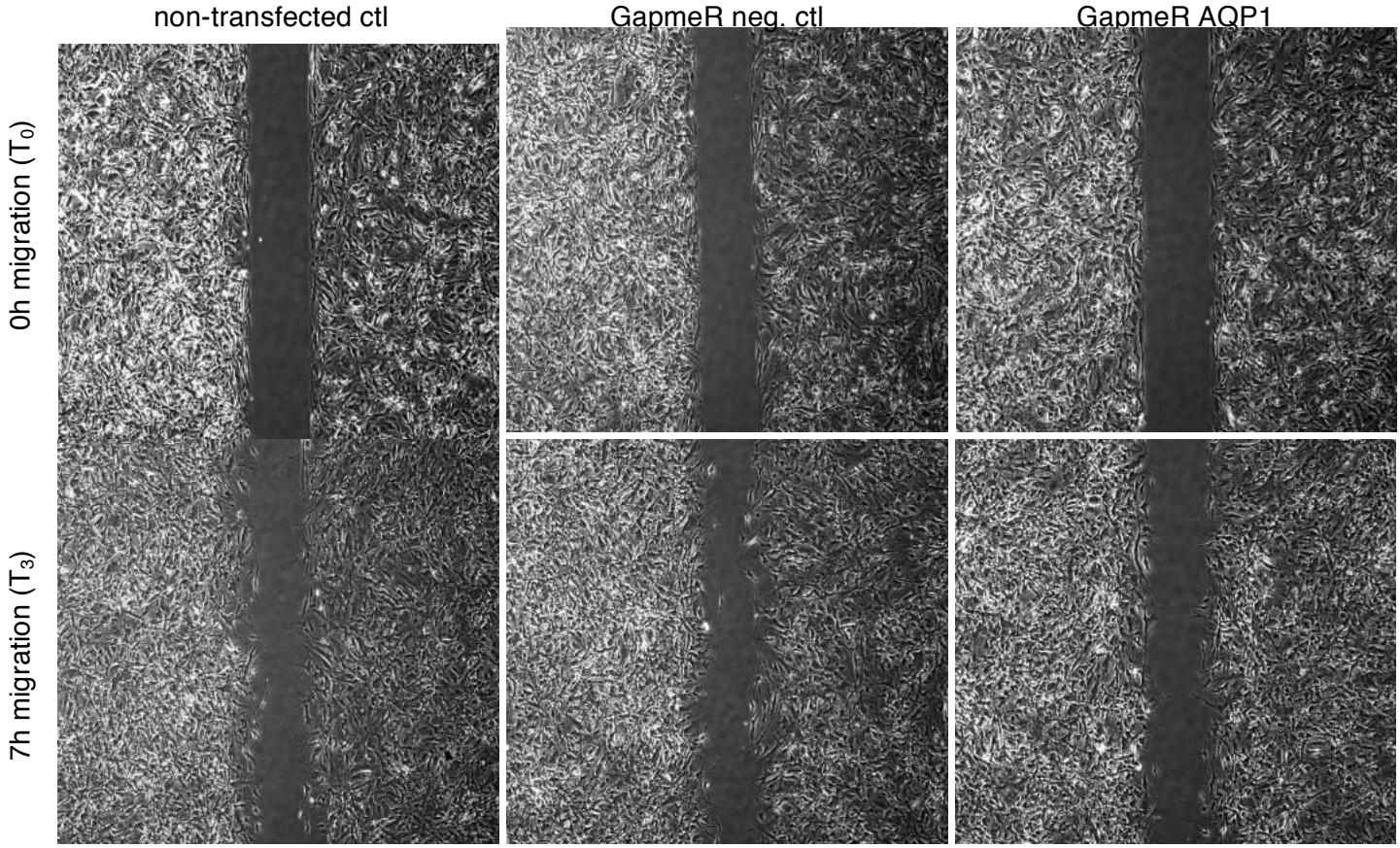

Donor #2

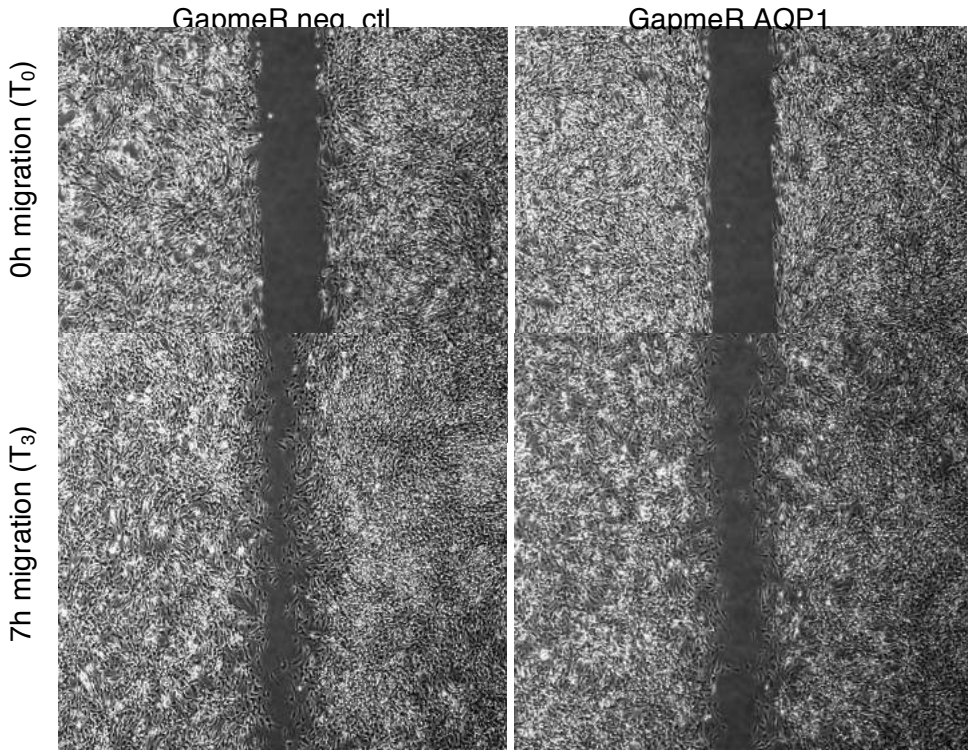

Supplementary Figure 2: Representative pictures of HPASMC migrated for 7h in hypoxia (Hx) after transfection with GapmeR targeting AQP1 compared to non-transfected or GapmeR negative control transfected cells.

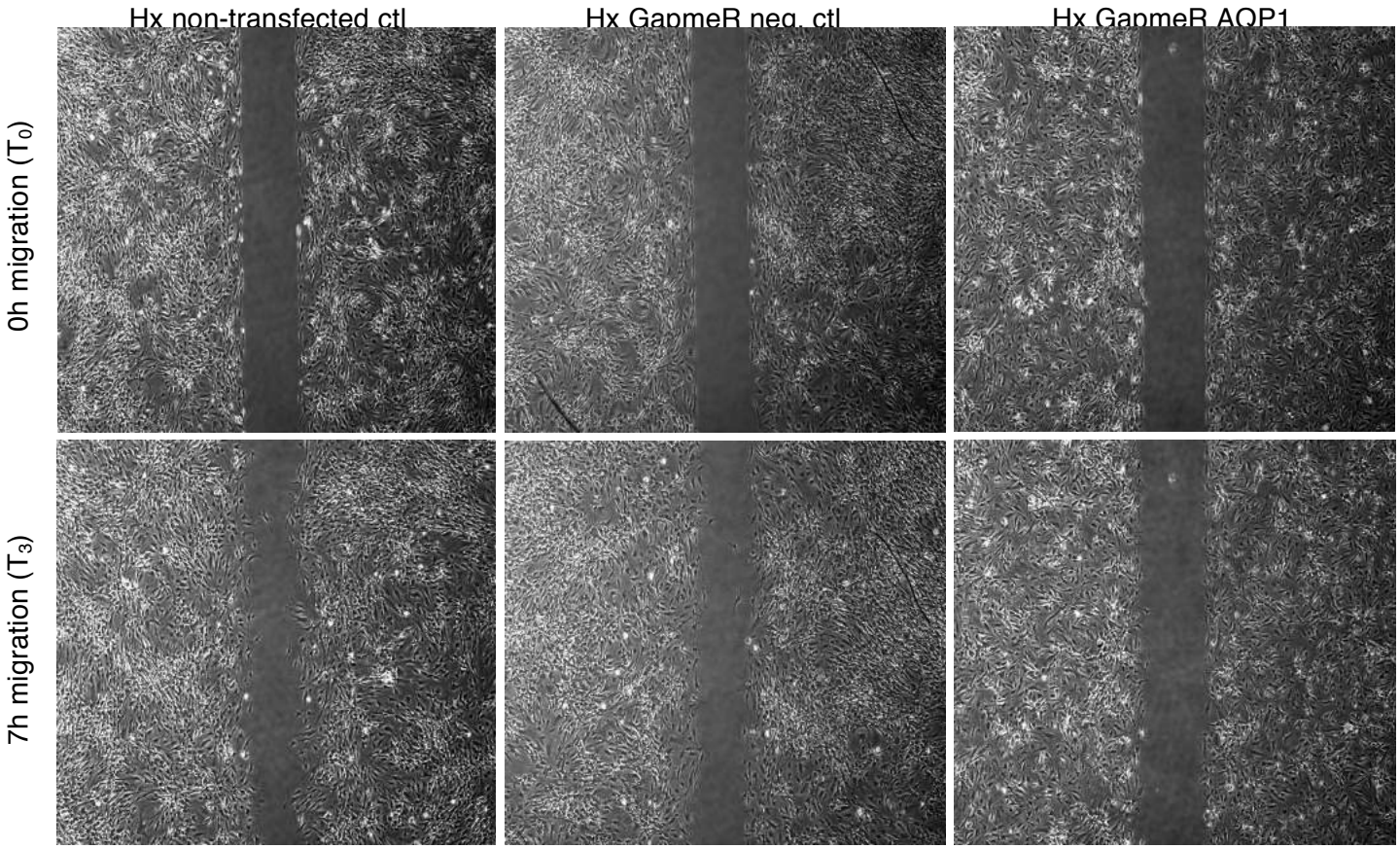

Supplementary Figure 3: Representative pictures of HPASMC migrated for 7h after transfection with AQP1 overexpressing vector (pcDNA_AQP1) compared to empty control transfected cells (pcDNA_empty).